Dual action of ketamine confines addiction liability

Simmler, Linda; Li, Yue; Hadjas, Lotfi; Hiver, Agnès; Van Zessen, Ruud; Luescher, Christian

How to cite

SIMMLER, Linda et al. Dual action of ketamine confines addiction liability. In: Nature, 2022, vol. 608, n° 7922, p. 368–373. doi: 10.1038/s41586-022-04993-7

This publication URL: https://archive-ouverte.unige.ch/unige:165984
Publication DOI: 10.1038/s41586-022-04993-7

Dual-action of ketamine confines addiction liability

Linda D. Simmler[1]*, Yue Li[1]*, Lotfi C. Hadjas[1], Agnès Hiver[1], Ruud van Zessen[1], and Christian Lüscher[1,2]

[1]*Department of Basic Neurosciences, University of Geneva, Rue Michel-Servet 1, 1206 Geneva, Switzerland,*

[2]*Service de Neurologie, Department of Clinical Neurosciences, Geneva University Hospital, Rue Gabrielle-Perret-Gentil 4, 1205 Geneva, Switzerland.*

**these authors contributed equally to this work*

Abstract

Ketamine is clinically used as an anesthetic, a fast-acting antidepressant and recreationally used for its dissociative properties. Addictive drugs, such as cocaine, increase dopamine (DA) levels in the nucleus accumbens (NAc). This facilitates synaptic plasticity in the mesolimbic system, which causes behavioral adaptations, eventually driving the transition to compulsion[1-4]. The addiction liability of ketamine is a matter of much debate, also because of its complex pharmacology that among several targets includes N-methyl-d-aspartic acid (NMDA) receptor (NMDAR) antagonism[5,6]. Here we show that ketamine fails to induce synaptic plasticity typically observed with addictive drugs in mice despite inducing robust DA transients in the NAc. Ketamine nevertheless supported reinforcement via disinhibition of DA neurons in the ventral tegmental area (VTA). This effect was mediated by NMDAR antagonism in VTA γ-aminobutyric acid (GABA) neurons, but quickly terminated by type 2 DA receptors (D_2R) on DA neurons. The rapid off-kinetics of the DA transients along with the NMDARs antagonism precluded the induction of synaptic plasticity in the VTA and NAc, and failed to elicit locomotor sensitization and uncontrolled self-administration. In summary, ketamine's dual-action leads to a unique constellation for DA-driven positive reinforcement, yet low addiction liability.

Main

Ketamine is a club drug classified as a schedule III substance for its putative addiction liability. While currently rarely used as anesthetic, the debate to which extent ketamine can cause loss of control and compulsion has re-emerged now that the molecule is more widely used as a fast-acting antidepressant. Rodent studies suggest a risk for addiction because early microdialysis studies revealed a general elevation of DA in the NAc[7-9], a hallmark of addictive drugs, including cocaine[4]. Moreover, behavioral studies suggest that ketamine is rewarding and reinforcing in rats[10-13], also a commonality of addictive drugs. The pharmacological targets of ketamine are many[6], with the highest affinity for NMDARs (antagonist)[5]. The long-term effects of ketamine on mesolimbic reward circuits and behavior however remain elusive. For example, we do not know whether ketamine induces synaptic plasticity typically evoked by addictive drugs, which drive early adaptive behavior and eventually compulsion[14,15]. Cocaine, already after the first dose potentiates glutamate synapses onto DA neurons in the VTA[16], expressed by the insertion of Ca^{2+}-permeable α-amino-3-hydroxy-5-methyl-4-isoxazolepropionic acid (AMPA) receptors (AMPARs)[17,18]. This receptor redistribution in the VTA serves as a permissive metaplasticity, which, with repeated drug exposure, reflects in a strengthening of excitatory synapses onto D_1-receptor expressing medium spiny neurons (D1-MSNs) in the NAc[19-21] and eventually synaptic plasticity in the dorsal striatum[22]. Here we investigate whether ketamine increases mesolimbic DA with latest generation fluorescent transmitter and activity indicators, and assess its effects on synapses and behavior.

Results

Reinforcement & DA elevation in the NAc

In an open field, a single dose of 30 mg/kg ketamine enhanced locomotion similar to cocaine (15 mg/kg; Fig. 1a, b). We next tested the rewarding and reinforcing properties of ketamine (Fig. 1c). Mice readily self-administered the drug (1 mg/kg/infusion in a 2h short access protocol) taking a number of infusion comparable to cocaine (0.75 mg/kg/infusion; Fig. 1d, e, Extended Data Fig. 1). Given this behavioral hallmark, we measured DA using a genetically encoded DA sensor (dLight1.1, Fig.1f). A single intraperitoneal (i.p.) injection of ketamine elicited DA transients in the NAc similar in magnitude, but of shorter duration than cocaine (Fig. 1g). The DA transients' area under the curve increased in a dose-dependent manner (Extended Data Fig. 2).

VTA DA neuron disinhibition

To test the effects on neuronal activity we monitored the fluorescence of a genetically encoded Ca^{2+} sensor (GCaMP6m, Fig. 2a) in DA and GABA neurons of the VTA. Ketamine increased DA neuron activity for 5 min after i.p. injection (Fig. 2b), consistent with the fast kinetics observed for DA release in the NAc (Fig. 1g). By contrast and as expected, cocaine decreased VTA DA neuron activity (Fig. 2b) due to activation of inhibitory D_2 autoreceptors[23]. In GABA neurons, we observed that ketamine induced a strong and sustained inhibition (Fig. 2c), while cocaine did not affect VTA GABA neuron activity. This suggests a primary inhibition of VTA GABA neurons that may cause a disinhibition, but raises questions why VTA DA GCaMP6m and NAc dLight signals show a short-lived signal change after ketamine injections.

We first confirmed whether NMDARs expressed on VTA GABA cells are indeed the primary targets of ketamine. We removed the NMDARs by deleting the obligatory subunit NR1 (*Grin1*)

selectively from VTA GABA cells (Fig. 2d; validated by decreased NMDA/AMPA ratios, see Extended Data Fig. 3) using a Cre-dependent CRISPR/SaCas9 knock-out (KO) strategy[24] in VGat-Cre mice. This led to the loss of ketamine's effect on VTA GABA neuron activity (Fig. 2e) but did not affect fentanyl induced GABA inhibition (Extended Data Fig. 4a, b). As a result, ketamine-evoked DA release in the NAc in VTA-GABA NR1-KO was reduced (Fig. 2f, g). The deletion of NMDARs in GABA neurons had also a small effect on cocaine elicited DA transients (Extended Data Fig. 4e-g), possibly because of an enhanced baseline activity of DA neurons. The disinhibitory motif of ketamine's circuit effects is further supported by the effect of ketamine on optogenetic VTA GABA neuron inhibition, which is also reinforcing[25]. To this end, we expressed the inhibitory opsin eArch3.0 in VTA GABA neurons and measured DA transients in the NAc (Fig. 2h, i). We delivered 30 laser pulses of 10 s duration on the first day and injected a dose of ketamine (45 mg/kg i.p.) after the first 5 pulses on the second day (Fig. 2i). We observed that the laser-induced DA transients in the NAc became smaller with ketamine treatment (Fig. 2j). This partial occlusion of laser-induced disinhibition through a non-saturating dose of ketamine corroborates the VTA-specific disinhibitory motif for ketamine action on the DA system.

We next addressed the decay kinetics in DA neurons despite continued VTA GABA inhibition (Fig. 2c). In fact, ketamine-evoked DA transients (Fig. 1g) and DA neuron activity (Fig. 2b) decayed within minutes. This is in contrast to fentanyl, which caused a long-lasting only slowly decaying NAc DA transient through disinhibition (Extended Data Fig. 4a-d). To explore possible additional inhibitory mechanisms, we monitored DA neuron activity after fluphenazine-N-mustard (FNM; Fig. 3a, b) treatment. This irreversible D_2R antagonist extended the DA neuron activity in response to ketamine (Fig. 3c) and also reduced cocaine-induced DA neuron auto-inhibition (Fig. 3d). None of the interventions however were

100 complete, most likely reflecting inter-individual variance in FNM effect, as we found a
101 correlation of the FNM effect size for both, ketamine and cocaine, in a given individual (Fig.
102 3e).
103
104 *Fast off kinetics and NMDAR antagonism*
105 We next screened for a form of synaptic plasticity that appears already after a first injection of
106 an addictive drug[16] by testing for the presence of Ca^{2+}-permeable AMPARs in VTA DA
107 neurons. Ketamine did not induce inward rectification typical for the presence of such non-
108 canonical AMPARs, in contrast to cocaine (Fig. 3f, g). To parse the temporal requirement for
109 plasticity induction, we applied optogenetic activation of DA neurons *in vivo* of increasing
110 duration (Fig. 3h). While 15 min of stimulation left the synapses unchanged, we found that 60
111 min stimulation increased the rectification index (RI, Fig. 3i), similar to the 2 h stimulation
112 reported previously[18]. This explains, why in the case of ketamine i.p. injection, activation of
113 DA neurons for only a few minutes (Fig. 2b) was insufficient to induce plasticity.
114 The previous results suggest that the duration of DA neuron activation is a crucial predictor for
115 synaptic plasticity induced by 'drugs of abuse'. So next we investigated what would happen if
116 ketamine acted on DA neurons for a longer period, by repeatedly injecting ketamine. To
117 generate such a drug-regimen, we intravenously (i.v.) infused ketamine or cocaine every 2 or
118 4 minutes (based on self-administration; Extended Data Fig. 1d; ketamine 1 mg/kg/infusion,
119 cocaine 0.75 mg/kg/infusion) for 2 h to generate DA elevation in the NAc of comparable
120 magnitude and duration (Fig. 3j, k). While for cocaine this protocol increased the RI at
121 excitatory synapses onto VTA DA neurons, ketamine failed to do so (Fig. 3l). Thus, an
122 additional mechanism may be involved to explain ketamine's lack of effect on synaptic
123 plasticity. This could be ketamine antagonizing NMDARs since, in addition to DA elevation,
124 activation of NMDARs is required for the potentiation of excitatory synapses onto VTA DA

neurons as well as D1R-MSNs[26]. Indeed, in patch-clamp experiments, the application of ketamine in a concentration (50 µM) corresponding to expected brain levels in mice[27-29] strongly inhibited NMDAR-mediated synaptic currents (Extended Data Fig. 5). As a result, ketamine also blocked long-term potentiation in acute brain slices (Fig. 3m). Thus, in repeated drug application regimens where the rapid off-kinetics of ketamine-induced DA effects are overcome, ketamine's NMDAR antagonism still prevents the induction of synaptic plasticity typically observed with addictive drugs.

No accumbal drug-evoked plasticity

As increased expression of c-Fos in NAc D1-MSNs is an early indication for drug-evoked plasticity[30-32], we quantified c-Fos after a single injection of ketamine. Unlike cocaine, there was no increase of c-Fos positive D1-MSNs with ketamine (Fig. 4a-c). We next tested for locomotor sensitization as an early drug-adaptive behavior. We injected mice for five days, followed by withdrawal and re-exposure. For the initial 4-5 daily injections we observed a short-term sensitization for ketamine and cocaine (Fig. 4d-f). However, when tested after seven and 30 days of withdrawal, ketamine yielded a locomotor response similar to baseline, whereas sensitization persisted in cocaine-treated mice (Fig. 4d-f). In a separate cohort, after 14 days of withdrawal no drug-evoked synaptic plasticity was observed with ketamine, as RI and AMPA/NMDA ratio were comparable to saline-treated mice (Fig. 4g-i). By contrast, but in line with previous reports[33,34], cocaine increased the RI at mPFC-to-NAc D1-MSN synapses while the AMPA/NMDA ratio decreased (Fig. 4g-i). In an attempt to test for addiction criteria typically reached only by a subset of self-administering animals[35], we allowed for daily 4 h long access to ketamine, increasing the lever press ratio (fixed ratio, FR) every four days. While this confirmed the reinforcing nature of ketamine (Fig 1d), we observed that mice reduced self-administration once FR2 was introduced (Fig 4j, k). When compared to cocaine self-

administration, the number of infusions and active lever presses for ketamine was lower (Fig 4j, k). As a consequence the breakpoint in a progressive ratio schedule was also lower than what we observed with cocaine (Fig 4l), speaking to the low motivation for ketamine self-administration. The sporadic lever presses at the end of the schedule, was readily suppressed by the introduction of aversive air-puffs (Extended Data Fig. 6a). Air-puffs were chosen because of the slight analgesic effect of ketamine (Fig. 6b). These experiments highlight the absence of ketamine-evoked synaptic plasticity, and the failure to induce long-term locomotor sensitization or uncontrolled self-administration despite initial reinforcing effects.

Discussion

Here, we show that subanesthetic doses of ketamine increase VTA DA neuron activity by inhibiting NMDARs in VTA GABA neurons. This elicits a DA transient in the NAc that is terminated within minutes because D_2Rs become activated. Like cocaine, ketamine reinforces initial self-administration. However, unlike cocaine, ketamine does not evoke drug-adaptive synaptic plasticity, long-term locomotor sensitization, or uncontrolled self-administration. We argue that D_2R-mediated rapid off-kinetics and NMDAR antagonism preclude the potentiation of excitatory synapses in the VTA and NAc, thus limiting addiction liability.

The disinhibitory action of ketamine is reminiscent of the mechanism of action of opioids[25], benzodiazepines[36], γ-hydroxybutyrate (GHB)[37], and cannabinoids[38], which also inhibit VTA GABA interneurons. Ketamine is however unique as the decrease of VTA GABA activity is caused by the loss of NMDAR excitation. As in interneurons elsewhere, NMDARs on VTA GABA neurons contribute to excitatory transmission at resting potential, maybe through receptors of non-canonical subunit composition[39]. A similar disinhibitory motif has been proposed in the mPFC, where ketamine also inhibits GABA interneurons, such that pyramidal cell activity is disinhibited[40,41]. The DA neuron activity is terminated by D_2Rs [42], which activate G protein-gated inwardly rectifying potassium (GIRK) ion channel family, thus hyperpolarizing VTA DA neurons[43]. This could be a direct effect as ketamine has been shown to act as D_2R agonist with a K_i of 0.5 μM[42] (but see Can *et al.*[44]). Alternatively it could be the consequence of dendritic release of DA, as it is the case with cocaine[23]. However, fentanyl-induced DA release, which also occurs through disinhibition, has slower off-kinetics than ketamine. This difference would suggest a direct action of ketamine on D2Rs, which however remains controversial.

Many forms of drug-evoked synaptic plasticity require NMDARs for induction[45]. Moreover there is hierarchical organization as plasticity in the VTA[16] is permissive for plasticity in the NAc[1,21] and eventually in the dorsal striatum[22]. Early drug-adaptive synaptic plasticity underlies drug seeking[33], compulsive drug taking[22] and locomotor sensitization[34]. With ketamine, we observed neither synaptic plasticity in the mesolimbic DA system nor long-term locomotor sensitization. This is in line with previous reports of some degree of short-term sensitization[46,47]. Early forms of drug-evoked plasticity are necessary to engage circuit organizations eventually underlying compulsive drug seeking and drug taking[15]. As our data indicate the absence of uncontrolled ketamine self-administration, this strongly suggests that ketamine's addiction liability is low.

The lack of drug-evoked synaptic plasticity has two reasons. First, with a single dose, because of its fast off-kinetics, the DA elevation was insufficient to cause plasticity in the VTA. Second, with repeated i.v. infusions causing longer-lasting DA elevation, NMDAR blockade prevented plasticity. The dual-action revealed here are relevant for therapy in humans. To treat depression, ketamine or its enantiomer S-ketamine are administered in sub-anesthetic doses either as 40-min i.v. infusion (0.5 mg/kg)[48] or as nasal spray (Esketamine; 56-84 mg) on a maximal bi-weekly basis. Since the nasal spray causes a rapid ketamine exposure similar to i.p. injections in our animal model, the fast off kinetics of accumbal DA in combination with NMDAR blockade may preclude drug-evoked synaptic plasticity. Even with repetitive i.v. infusions causing prolonged enhanced DA levels, NMDAR blockade may still confine drug-adaptive plasticity.

Overall, we found that ketamine has rewarding and reinforcing properties since it indirectly acts on the DA system via circuit effects from local GABA neurons. The absence of drug-

adaptive synaptic plasticity in the mesolimbic system strongly indicates that ketamine's addiction liability is limited by its pharmacology, as D_2R-mediated VTA DA neuron inhibition explains the fast off-kinetics and NMDAR antagonism prevents induction mechanisms for synaptic changes. The insight into ketamine's acute and chronic effects on the mesolimbic DA system may guide the consensus for access to treatment for clinical indications, such as depression.

References

1 Bellone, C., Loureiro, M. & Luscher, C. Drug-evoked wynaptic plasticity of excitatory transmission in the ventral tegmental area. *Cold Spring Harb Perspect Med* **11**, doi:10.1101/cshperspect.a039701 (2021).

2 Di Chiara, G. *et al.* Dopamine and drug addiction: the nucleus accumbens shell connection. *Neuropharmacology* **47 Suppl 1**, 227-241, doi:10.1016/j.neuropharm.2004.06.032 (2004).

3 Lüscher, C., Robbins, T. W. & Everitt, B. J. The transition to compulsion in addiction. *Nat Rev Neurosci* **21**, 247-263, doi:10.1038/s41583-020-0289-z (2020).

4 Lüscher, C. & Ungless, M. A. The mechanistic classification of addictive drugs. *PLoS Med* **3**, e437, doi:10.1371/journal.pmed.0030437 (2006).

5 Franks, N. P. & Lieb, W. R. Molecular and cellular mechanisms of general anaesthesia. *Nature* **367**, 607-614, doi:10.1038/367607a0 (1994).

6 Zanos, P. *et al.* Ketamine and ketamine metabolite pharmacology: insights into therapeutic mechanisms. *Pharmacol Rev* **70**, 621-660, doi:10.1124/pr.117.015198 (2018).

7 Masuzawa, M. *et al.* Pentobarbital inhibits ketamine-induced dopamine release in the rat nucleus accumbens: a microdialysis study. *Anesth Analg* **96**, 148-152, table of contents, doi:10.1097/00000539-200301000-00030 (2003).

8 Witkin, J. M. *et al.* The rapidly acting antidepressant ketamine and the mGlu2/3 receptor antagonist LY341495 rapidly engage dopaminergic mood circuits. *J Pharmacol Exp Ther* **358**, 71-82, doi:10.1124/jpet.116.233627 (2016).

9 Littlewood, C. L. *et al.* Mapping the central effects of ketamine in the rat using pharmacological MRI. *Psychopharmacology (Berl)* **186**, 64-81, doi:10.1007/s00213-006-0344-0 (2006).

10 Rocha, B. A., Ward, A. S., Egilmez, Y., Lytle, D. A. & Emmett-Oglesby, M. W. Tolerance to the discriminative stimulus and reinforcing effects of ketamine. *Behav Pharmacol* **7**, 160-168 (1996).

11 De Luca, M. T. & Badiani, A. Ketamine self-administration in the rat: evidence for a critical role of setting. *Psychopharmacology (Berl)* **214**, 549-556, doi:10.1007/s00213-010-2062-x (2011).

12 Zanos, P. *et al.* A negative allosteric modulator for alpha5 subunit-containing GABA receptors exerts a rapid and persistent antidepressant-like action without the side effects of the NMDA receptor antagonist ketamine in mice. *eNeuro* **4**, doi:10.1523/ENEURO.0285-16.2017 (2017).

13 Suzuki, T. *et al.* Effects of the non-competitive NMDA receptor antagonist ketamine on morphine-induced place preference in mice. *Life Sci* **67**, 383-389, doi:10.1016/s0024-3205(00)00639-1 (2000).

14 Luscher, C. & Malenka, R. C. Drug-evoked synaptic plasticity in addiction: from molecular changes to circuit remodeling. *Neuron* **69**, 650-663, doi:10.1016/j.neuron.2011.01.017 (2011).

15 Luscher, C. The emergence of a circuit model for addiction. *Annu Rev Neurosci* **39**, 257-276, doi:10.1146/annurev-neuro-070815-013920 (2016).

16 Ungless, M. A., Whistler, J. L., Malenka, R. C. & Bonci, A. Single cocaine exposure in vivo induces long-term potentiation in dopamine neurons. *Nature* **411**, 583-587, doi:10.1038/35079077 (2001).

17 Bellone, C. & Luscher, C. Cocaine triggered AMPA receptor redistribution is reversed in vivo by mGluR-dependent long-term depression. *Nature neuroscience* **9**, 636-641, doi:10.1038/nn1682 (2006).

18 Brown, M. T. *et al.* Drug-driven AMPA receptor redistribution mimicked by selective dopamine neuron stimulation. *PloS one* **5**, e15870, doi:10.1371/journal.pone.0015870 (2010).

19 Conrad, K. L. *et al.* Formation of accumbens GluR2-lacking AMPA receptors mediates incubation of cocaine craving. *Nature* **454**, 118-121, doi:10.1038/nature06995 (2008).

20 Kourrich, S., Rothwell, P. E., Klug, J. R. & Thomas, M. J. Cocaine experience controls bidirectional synaptic plasticity in the nucleus accumbens. *J Neurosci* **27**, 7921-7928, doi:10.1523/JNEUROSCI.1859-07.2007 (2007).

21 Mameli, M. *et al.* Cocaine-evoked synaptic plasticity: persistence in the VTA triggers adaptations in the NAc. *Nature neuroscience* **12**, 1036-1041, doi:10.1038/nn.2367 (2009).

22 Pascoli, V. *et al.* Stochastic synaptic plasticity underlying compulsion in a model of addiction. *Nature* **564**, 366-371, doi:10.1038/s41586-018-0789-4 (2018).

23 Brodie, M. S. & Dunwiddie, T. V. Cocaine effects in the ventral tegmental area: evidence for an indirect dopaminergic mechanism of action. *Naunyn Schmiedebergs Arch Pharmacol* **342**, 660-665, doi:10.1007/BF00175709 (1990).

24 Hunker, A. C. *et al.* Conditional single vector CRISPR/SaCas9 viruses for efficient mutagenesis in the adult mouse nervous system. *Cell Rep* **30**, 4303-4316 e4306, doi:10.1016/j.celrep.2020.02.092 (2020).

25 Corre, J. *et al.* Dopamine neurons projecting to medial shell of the nucleus accumbens drive heroin reinforcement. *Elife* **7**, doi:10.7554/eLife.39945 (2018).

26 Luscher, C. & Malenka, R. C. NMDA receptor-dependent long-term potentiation and long-term depression (LTP/LTD). *Cold Spring Harb Perspect Biol* **4**, a005710, doi:10.1101/cshperspect.a005710 (2012).

27 Zanos, P. *et al.* NMDAR inhibition-independent antidepressant actions of ketamine metabolites. *Nature* **533**, 481-486, doi:10.1038/nature17998 (2016).

28 Ganguly, S., Panetta, J. C., Roberts, J. K. & Schuetz, E. G. Ketamine pharmacokinetics and pharmacodynamics are altered by P-glycoprotein and breast cancer resistance protein efflux transporters in mice. *Drug Metab Dispos* **46**, 1014-1022, doi:10.1124/dmd.117.078360 (2018).

29 Saland, S. K. & Kabbaj, M. Sex differences in the pharmacokinetics of low-dose ketamine in plasma and brain of male and female rats. *J Pharmacol Exp Ther* **367**, 393-404, doi:10.1124/jpet.118.251652 (2018).

30 Valjent, E. *et al.* Involvement of the extracellular signal-regulated kinase cascade for cocaine-rewarding properties. *J Neurosci* **20**, 8701-8709 (2000).

31 Valjent, E. *et al.* Regulation of a protein phosphatase cascade allows convergent dopamine and glutamate signals to activate ERK in the striatum. *Proc Natl Acad Sci U S A* **102**, 491-496, doi:10.1073/pnas.0408305102 (2005).

32 Bertran-Gonzalez, J. *et al.* Opposing patterns of signaling activation in dopamine D1 and D2 receptor-expressing striatal neurons in response to cocaine and haloperidol. *J Neurosci* **28**, 5671-5685, doi:10.1523/JNEUROSCI.1039-08.2008 (2008).

33 Pascoli, V. *et al.* Contrasting forms of cocaine-evoked plasticity control components of relapse. *Nature* **509**, 459-464, doi:10.1038/nature13257 (2014).

34 Pascoli, V., Turiault, M. & Luscher, C. Reversal of cocaine-evoked synaptic potentiation resets drug-induced adaptive behaviour. *Nature* **481**, 71-75, doi:10.1038/nature10709 (2012).

35 Deroche-Gamonet, V., Belin, D. & Piazza, P. V. Evidence for addiction-like behavior in the rat. *Science* **305**, 1014-1017, doi:10.1126/science.1099020 (2004).

36 Tan, K. R. *et al.* Neural bases for addictive properties of benzodiazepines. *Nature* **463**, 769-774, doi:10.1038/nature08758 (2010).

37 Cruz, H. G. *et al.* Bi-directional effects of GABA(B) receptor agonists on the mesolimbic dopamine system. *Nature neuroscience* **7**, 153-159, doi:10.1038/nn1181 (2004).

38 Melis, M. *et al.* Endocannabinoids mediate presynaptic inhibition of glutamatergic transmission in rat ventral tegmental area dopamine neurons through activation of CB1 receptors. *J Neurosci* **24**, 53-62, doi:10.1523/JNEUROSCI.4503-03.2004 (2004).

39 Paoletti, P., Bellone, C. & Zhou, Q. NMDA receptor subunit diversity: impact on receptor properties, synaptic plasticity and disease. *Nat Rev Neurosci* **14**, 383-400, doi:10.1038/nrn3504 (2013).

40 Moghaddam, B., Adams, B., Verma, A. & Daly, D. Activation of glutamatergic neurotransmission by ketamine: a novel step in the pathway from NMDA receptor blockade to dopaminergic and cognitive disruptions associated with the prefrontal cortex. *J Neurosci* **17**, 2921-2927 (1997).

41 Ali, F. *et al.* Ketamine disinhibits dendrites and enhances calcium signals in prefrontal dendritic spines. *Nat Commun* **11**, 72, doi:10.1038/s41467-019-13809-8 (2020).

42 Kapur, S. & Seeman, P. NMDA receptor antagonists ketamine and PCP have direct effects on the dopamine D(2) and serotonin 5-HT(2)receptors-implications for models of schizophrenia. *Mol Psychiatry* **7**, 837-844, doi:10.1038/sj.mp.4001093 (2002).

43 Luscher, C. & Slesinger, P. A. Emerging roles for G protein-gated inwardly rectifying potassium (GIRK) channels in health and disease. *Nat Rev Neurosci* **11**, 301-315, doi:10.1038/nrn2834 (2010).

44 Can, A. *et al.* Effects of ketamine and ketamine metabolites on evoked striatal dopamine release, dopamine receptors, and monoamine transporters. *J Pharmacol Exp Ther* **359**, 159-170, doi:10.1124/jpet.116.235838 (2016).

45 Engblom, D. *et al.* Glutamate receptors on dopamine neurons control the persistence of cocaine seeking. *Neuron* **59**, 497-508, doi:10.1016/j.neuron.2008.07.010 (2008).

46 Uchihashi, Y., Kuribara, H., Morita, T. & Fujita, T. The repeated administration of ketamine induces an enhancement of its stimulant action in mice. *Japanese journal of pharmacology* **61**, 149-151, doi:10.1254/jjp.61.149 (1993).

47 Wiley, J. L., Evans, R. L., Grainger, D. B. & Nicholson, K. L. Age-dependent differences in sensitivity and sensitization to cannabinoids and 'club drugs' in male adolescent and adult rats. *Addiction biology* **13**, 277-286, doi:10.1111/j.1369-1600.2007.00077.x (2008).

48 Berman, R. M. *et al.* Antidepressant effects of ketamine in depressed patients. *Biol Psychiatry* **47**, 351-354, doi:10.1016/s0006-3223(99)00230-9 (2000).

Fig. 1 | Ketamine causing hyperlocomotion, reinforcement, and DA elevation in the NAc. **a,** Top: Experimental timeline. Bottom: Representative track plots post i.p. injections. **b,** Distance travelled before and after i.p. injections. N (mice) = 7 (saline), 11 (ketamine), 11 (cocaine). **c,** Schematic of self-administration apparatus. **d,** Number of infusions in 2 h across the 10 sessions taken by mice self-administering saline, ketamine (1 mg/kg/infusion), or cocaine (0.75 mg/kg/infusion). N (mice) = 8 (saline), 10 (ketamine), 8 (cocaine). **e,** Number of infusions averaged across the 10 self-administration sessions. N (mice) = 8 (saline), 10 (ketamine), 8 (cocaine). **f,** Left: Schematic of virus injection and fiber implantation. Right: Representative picture of dLight expression. Scale bar, 500 μm. **g,** Average NAc dLight response to i.p. injections, N = 12 mice. Data are presented as mean ± SEM. **P < 0.01. For all i.p. injections, doses were 30 mg/kg ketamine and 15 mg/kg cocaine.

Fig. 2 | Accumbal DA transients are mediated by disinhibition of VTA DA neurons. a, Top: Schematic of virus injection and fiber implantation. Bottom: GCaMP6m expression (green) and TH immunostaining (red). Scale bars, 10 μm. **b,** Mean Ca^{2+} signal of VTA DA neurons with i.p. injections of saline, ketamine (30 mg/kg), and cocaine (15 mg/kg). N = 10 mice. **c,** Mean Ca^{2+} signal in VTA GABA neurons with i.p. injections, N = 7 mice. **d, f, h,** Experimental details. **e,** Mean Ca^{2+} signal of VTA GABA neurons from NR1-control (CT) and KO mice with i.p. injections of ketamine. N (mice) = 8 (CT) and 8 (KO). **g,** Area under curve of ketamine induced DA transients in NR1-CT and KO mice. N (mice) = 11 (CT) and 11 (KO). **i,** Representative dLight responses to eArch3.0 stimulation from sessions without (top) and with ketamine (45 mg/kg i.p.; bottom). **j,** ΔF/F during eArch3.0 stimulation normalized to the first 5 trials. N = 18 mice. Data are presented as mean ± SEM. **P < 0.01, ****P < 0.0001.

Fig. 3 | D_2R-mediated fast off-kinetics of DA transients and lack of early-adaptive synaptic plasticity. a, b, h, j, Experimental details. **c,** Left: Mean Ca^{2+} signal of VTA DA neurons with i.p. injections of saline, ketamine (30 mg/kg) and FNM (10 mg/kg) x ketamine. Right: Area under curve (AUC) of ketamine induced signal without and with FNM pre-treatment. N = 16 mice. **d,** Left: Mean Ca^{2+} signal of VTA DA neurons with i.p. injections of saline, cocaine (15 mg/kg) and FNM x cocaine. Right: AUC cocaine induced signal without and with FNM pre-treatment. N = 16 mice. Saline trace is the same as in **c** because conditions were assessed consecutively (**b**). **e,** Differences of AUC between cocaine- and FNM x cocaine-induced signal as a function of differences of AUC between ketamine- and FNM x ketamine-induced signal. **f,** Top: Experimental details. Bottom: Example traces of AMPAR currents used to calculate RI. Scale bars, 10 ms, 100 pA. **g,** RI of putative VTA DA neurons. N (cells) = 7 (saline), 7 (ketamine), 8 (cocaine). **i,** RI in VTA DA neurons. N (cells) = 5 (0 min), 7 (15 min), 7 (60 min). **k,** Mean NAc dLight response to i.v. infusions of saline and ketamine (1 mg/kg/infusion) every 2 min and cocaine (0.75 mg/kg/infusion) every 4 min. N (mice) = 4 (saline), 7 (ketamine), 7 (cocaine). **l,** Left: experimental details. Right: RI in putative VTA DA neurons. N (cells) = 7 (saline), 13 (ketamine), 11 (cocaine). **m,** Long-term potentiation induced in NAc slices with high-frequency stimulation (HFS). Left: Time-course of normalized EPSCs with and without 50 μM ketamine. Right: Normalized EPSCs averaged across the last 10 min.

N (cells) = 10 (control), 8 (ketamine). Data are presented as mean ± SEM. *P < 0.05, **P < 0.01, ***P < 0.001.

Fig. 4 | Absence of accumbal drug-evoked synaptic plasticity, locomotor sensitization, and uncontrolled self-administration. a, Left, experimental timeline. Right, brain area for imaging. **b,** Representative confocal images of NAc shell expressing c-Fos. White arrows point to D1-MSNs expressing c-Fos. Scale bars, 50 µm. **c**, Average cell density per mouse for c-Fos$^+$/tdTomato$^+$ cells in the NAc shell. N(mice) = 4 (ketamine), 5 (cocaine), 4 (saline). **d,** Paradigm for locomotor sensitization. **e,** Distance travelled after i.p. injection normalized to the first day of drug administration. N (mice) = 11 (ketamine), 10 (cocaine). **f,** Sensitization index calculated for day 5 (D5/D1), day 21 (D12/D1), and day 36 (D36/D1). N (mice) = 11 (ketamine), 10 (cocaine). **g,** Experimental details. Bottom right image: green, ChR2 infection site; orange, tdTomato$^+$ D1-MSNs; blue, DAPI. Scale bar, 500 µm. **h,** Example traces for RI (top) and AMPA/NMDA (bottom). Scale bars, 50 ms, 100 pA. **i,** Left: RI and Right: AMPA/NMDA in NAc D1-MSNs. For RI: N (cells) = 16 (saline), 18 (ketamine), 16 (cocaine). For AMPA/NMDA: N (cells) = 16 (saline), 19 (ketamine), 17 (cocaine). **j,** Number of ketamine (1 mg/kg/infusion) and cocaine (0.5 mg/kg/infusion) infusions during acquisition. N (mice) = 20 (ketamine) and 12 (cocaine). **k.** Left, number of active and inactive lever presses during ketamine and cocaine self-administration across sessions. Right, preference for active lever (active minus inactive lever presses) on the last session. N (mice) = 20 (ketamine) and 12 (cocaine). **l.** Break points of ketamine and cocaine self-administration. N (mice) = 20 (ketamine) and 10 (cocaine). Values are presented as mean ± SEM. *P < 0.05, **P < 0.01, ***P < 0.001, ****P < 0.0001. For all i.p. injections, doses were 30 mg/kg ketamine and 15 mg/kg cocaine.

Methods

Mice

C57BL/6J (wildtype) mice were purchased from Charles River. Drd1-Tomato (Tg(Drd1a-tdTomato)6Calak/J), DAT-Cre (Slc6a3tm1.1(cre)Bkmn), GAD-Cre (Gad2tm2(cre)Z) and VGat-Cre (Slc32a1tm2(cre)Lowl/J) mouse lines were from the Jackson Laboratory (USA). Male and female mice aged 3 – 20 weeks were used and housed with food and water *ad libitum* on a normal 12 h light-dark cycle (light on at 7:00 AM) with temperature (18-23°C) and humidity (40-60%) precisely controlled. Mice were group housed except for those used for self-administration experiments. All procedures were approved by the Institutional Animal Care and Use Committee of the University of Geneva and by the animal welfare committee of the Canton of Geneva, in accordance with Swiss law.

Drugs

A racemic mixture of ketamine was purchased as 50 mg/ml solution from Labatec (Switzerland). Cocaine-HCl was provided by the pharmacy of the University Hospital of Geneva. Fentanyl was purchased as 0.05 mg/ml solution from Sintetica (Switzerland). FNM (fluphenazine-N-2-chloroethane.2HCl) was from Enzo Life Sciences (Switzerland). For *in vivo* administration, ketamine and fentanyl solution were diluted with sterile 0.9% NaCl (saline). Cocaine and FNM were dissolved in saline. For i.v. administration, drug solutions were filtered (0.22 µm pore size).

Acute hyperlocomotion and behavioral sensitization

Mice were habituated to the behavior room, handling, and intraperitoneal (i.p.) injections on three days prior to testing. On testing days, mice underwent room habituation for a minimum of 1 h. Then, they were individually transferred into a testing arena (20 cm x 20 cm squared

box made of frosted opal-white acrylic glass). After 20 min of habituation to the arena, mice were i.p. injected and left in the arena for another 60 min. I.p. injections were saline (10 ml/kg), ketamine (30 mg/kg) or cocaine (15 mg/kg). For behavioral sensitization, injections (saline, ketamine or cocaine) were repeated daily for a total of 5 days. Drug challenge after home-cage withdrawal was tested after 7 and 30 days of withdrawal. Mice which were used for *ex vivo* patch-clamp experiments after sensitization underwent 10-14 days of withdrawal and were sacrificed for slice recordings instead of getting exposed to a drug challenge behavioral session. Locomotor activity was recorded and analysed using Anymaze version 4.95 (Stoelting). Sensitization index was calculated as total distance travelled in 30 min post injection after sensitization divided by the distance on day 1 of drug administration.

Drug self-administration

Jugular vein catheters were implanted under anesthesia with a ketamine-xylazine mixture (80 mg/kg and 10 mg/kg, respectively) one week before starting the experiment. After surgery, mice were singly-housed, treated with the antibiotic amikacin (10 mg/kg subcutaneously) for 5 days. Catheters were flushed daily with heparin (2.5 IE) after the surgery, before and after the self-administration sessions until the end of experiment.

Mice were mildly food deprived for one night before the first self-administration session to increase exploratory behavior. *Ad libitum* feeding resumed immediately after the first session. For the acquisition sessions, mice were placed individually into operant boxes with an active and an inactive lever (assignment counter-balanced between mice) and trained on a fixed ratio (FR) 1 schedule for figure 1c-e (first self-administration cohort), and increased FRs for figure 4j-l (second self-administration cohort). A press on the active lever turned on a cue light for 10 s (1-s on/off at 1 Hz) and the infusion of the assigned drug. There was a 20 s time-out after every infusion, during which lever pressing did not trigger any response. Infusions were

ketamine (1 mg/kg/infusion), cocaine (0.75 mg/kg/infusion for figure 1c-e, and 0.5 mg/kg/infusion for figure 4j-l), or saline (1 ml/kg/infusion). For the first self-administration cohort, sessions lasted maximal 120 min or were terminated earlier when 45 infusions were administered (short access). For the second self-administration cohort, sessions lasted for 240 min (long-access). After long-access sessions to ketamine, mice were subjected to 2 baseline and 3 punishment sessions, with each session lasted for 120 min. For punishment sessions, 1 s air puff (from two sides and above the mouse head) were conducted every 3 infusions. The experimental protocols were controlled and data were collected with MED-PC Ⅳ 4.34 (Med Associates).

Hotplate test

The mice were placed on the pre-heated (55 ± 0.2 ℃) hotplate apparatus 0.5-1 h before and immediately after i.v. infusions of saline or ketamine (1 mg/kg/infusion, 4 min interval, 30 infusions within 2 h). Latency to hotplate was calculated as the time between placing the mice and the first jump / hind paw withdrawal / lick / tremble. A 30 s cutoff was set to avoid tissue damage.

Stereotactic surgeries

Standard stereotactic surgeries were conducted under isoflurane anesthesia. GCaMP6m was from Stanford University vector core, dLight1.1 was from Addgene, and the NR1-KO and control viruses were provided by Dr. Larry Zweifel, University of Washington[24]. All other viruses were purchased from University of North Carolina vector core. Bregma and dura mater were used as reference points.

For the dLight experiments, AAV5-CAG-dLight1.1 (500 nl) was injected unilaterally at +1.5 AP, ±0.7 ML, -4.3 DV (NAc). For GCaMP experiments, AAV-DJ-EF1α-FLEX-GCaMP6m (500 nl) was injected at -3.2 AP, ±0.6 ML, -4.5 DV (VTA).

For cell-specific NR1-KO and the respective control, 300 nl of AAV1-CMV-FLEX-SaCas9-U6-sgGrin1 or AAV1-CMV-FLEX-SaCas9-U6-sgRosa26 were injected as 8:1 mixture with AAV1-FLEX-EGFP-KASH at -3.2 AP, ±0.6 ML, -4.5 DV (VTA). The KASH virus was omitted for the KO experiments with GCamp6m recording in the VTA. The CRISPR/Cas9 virus (plasmid available from Addgene) and guide RNA were generated and validated in detail in the Hunker study[24]. Briefly, a loxp-flanked *SaCas9* and a guide RNA under U6 promotor were inserted in the same vector. The guide RNA sequence was designed to target the most common exon of the gene according to online resources. The absence of GluN1 subunit was confirmed by sequencing after FACs and lack of NMDA currents in infected cells[24].

For inhibition of VTA GABA cells, AAV5-Ef1α-DIO-eArch3.0-eYFP (300 nl) was injected unilaterally at -3.2 AP, ±0.6 ML, -4.5 DV (VTA). Optic fibers were implanted unilaterally 0.2 – 0.3 mm more dorsal than virus injections, and fixed in head caps with dental cement and anchor screws.

For patch clamp experiments, AAV5-CamKIIα-ChR2(H134R)-eYFP (400 nl) was injected bilaterally at +1.9 AP, ±0.3 ML, -2.0 DV (mPFC). For *in vivo* stimulation of DA neurons, AAV5-Ef1α-DIO-ChR2(H134R)-mCherry (500 nl) was injected at -3.2 AP, ±0.9 ML, -4.5DV with a 10 ° angle (VTA). An optic fiber was implanted at -3.2 AP, ±0.9 ML, -4.3 DV with a 10 ° angle.

Fiber photometry

Fiber photometry experiments were performed as before[25]. Specifically, mice were habituated to the testing room, handling and i.p. injections for five days prior to testing. For testing, mice

were connected to the fiber photometry cable and placed in a circular arena (20 cm diameter) for 10 min of habituation. Then, 5 min of baseline fluorescence were recorded, followed by an i.p. drug or saline injection and another 20 – 30 min of recording.

Specific experimental condition: FNM (10 mg/kg i.p.) was injected 3 h before ketamine. For VTA GABA neuron inhibition in absence of drugs, a 5 min baseline was recorded, then an orange laser (593 nm, 10-15 mW) was turned on for 10 s every 1 min for 30 stimuli. For VTA GABA neuron inhibition in presence of ketamine, a 5 min baseline was recorded, then five 10-s laser stimuli were delivered, the ketamine (45 mg/kg) was i.p. injected and the first of 25 laser stimuli was started 60 s after i.p. injection. For data analysis of VTA GABA inhibition, traces were aligned to the onset of laser with a 10-s baseline. DeltaF/F values from the 10 s of baseline and 10 s during laser on were averaged, then amplitude was calculated by subtracting the baseline fluorescence from the laser-on fluorescence. Eventually the stimulation amplitude of the first five stimuli were averaged as well as stimuli #6-30, and the latter was normalized to stimuli #1-5.

Fiber photometry conditions: Fluorescent indicators were excited from two excitation sources, corresponding to 470 nm wavelength and 405 nm wavelength LED light (M470F3, M405FP1, Thorlabs). Excitation light was sinusoidally modulated and passed through excitation filters (FMC4_AE(405)_E(450-490)_F(500-550)_S) and onto an optic fiber patch cable (MFP_400/430/1100–0.48_4 m_FC-ZF2.5, Doric Lenses). The fiber patch cable was then connected to the chronically implanted optic fiber (MFC_400/430-0.48_6mm_ZF2.5(G)_FLT, Doric Lenses). Emission light travelled back through the same system, where it was filtered (500-550 nm wavelength) and acquired through a photoreceiver (Newport 2151). After pre-amplification by the photoreceiver (2×10^{10} V/A) the signal was digitized, demodulated and stored using a signal processor (RZ5P, Tucker Davis Technologies). Fiber photometry data were collected with TDT synapse version 84 (Tucker Davis), analysed using Matlab R2016b

(Mathworks). First, for the time before drug injection, the signal originating from the 405 nm excitation source was linearly regressed to the signal originating from the 470 nm excitation source. The regression coefficients are then applied to the entire 405 nm originating signal, scaling it to the 470 nm originating signal. ΔF/F was then computed as (470 nm signal – fitted 405 nm signal) / fitted 405 signal. Finally the ΔF/F was binned into appropriate time bins in the graphs and analyses.

In vivo stimulation of DA neurons

Ten to 14 days after surgery, mice were tethered to an optic fiber in their home cage for 1 h. They received laser stimulation for 0, 15, or 60 min. Laser stimulation (473 nm, 15 mW, 4 ms pulse duration) was delivered in bursts of 5 pulses at 20 Hz every 1 s[18]. Mice were sacrificed for patch-clamp recordings 24 h after stimulation.

Patch-clamp electrophysiology

For patch-clamp recordings, mice were sacrificed and brains were removed quickly. Brain slices of 220 µm thickness were cut in ice-cold artificial cerebrospinal fluid (aCSF; containing (in mM) 119 NaCl, 11 D-glucose, 26.2 $NaHCO_3$, 2.5 KCl, 1.3 $MgCl_2$, 1 NaH_2PO_4, 2.5 $CaCl_2$) and recovered for 15 min at 31 °C. For DA neurons, brains were cut in a cutting solution as described by Bariselli *et al.*[49]. The internal solution for whole-cell patch clamp contained (in mM) 130 CsCl, 4 NaCl, 5 creatine phosphate, 2 $MgCl_2$, 2 Na_2ATP, 0.6 Na_3GTP, 1.1 EGTA, 5 HEPES, 5 QX-314, 0.1 spermine, except for long-term potentiation (LTP) and NMDAR inhibition experiments which were conducted with internal solution containing (in mM) 140 K-gluconate, 10 creatine phosphate, 2 $MgCl_2$, 5 KCl, 4 Na_2ATP, 0.3 Na_3GTP, 0.2 EGTA, 10 HEPES. DA neurons were recorded with the same internal solution but without QX-314. Currents were evoked with blue light (470 nm LED, 1-4 ms pulse duration) or electrical

566 stimulation (100 µs pulse duration) in presence of 100 µM picrotoxin. Currents were amplified
567 (Multiclamp 700B, Axon Instruments), filtered at 2.2 kHz and digitized at 20 kHz (National
568 Instruments Board PCI-MIO-16E4, Igor, Wave Metrics). Data were collected with Igor 7
569 (Wave metrics). We did not correct for liquid junction potential (-3 mV). Cells were discarded
570 where series resistance changed by more than 20%.
571 For AMPA/NMDA ratios, recordings were performed at +40 mV holding potential without
572 and with 2-amino-5-phosphonopentanoic acid (AP-5; 50 µM) to obtain isolated AMPAR
573 currents and compute NMDAR currents from the combined AMPAR-NMDAR trace. For RI,
574 isolated AMPAR currents were recorded at -70, 0 and + 40 mV. For NMDAR inhibition
575 experiments, AMPARs were blocked with NBQX (10 µM) and Mg^{2+}-free aCSF was used. DA
576 cells were identified according to anatomical location, morphology, and cell capacitance[49]. In
577 the DA neuron stimulation experiment DA cells were identified by the presence of
578 photocurrents.
579 For in vitro LTP experiments, NAc slices from wildtype mice were incubated in Mg^{2+}-free
580 aCSF with or without 50 µM ketamine for 20-30 min, then recordings took place in normal
581 aCSF (containing 10 µM SKF38393 and 100 µM picrotoxin) with or without 50 µM ketamine.
582 LTP was induced with high-frequency stimulation (4 bursts of 100 stimuli at 100 Hz, 10 s
583 between bursts) with depolarization to 0 mV holding potential.
584 For GluN1 knockout validation, AAV1-FLEX-EGFP-KASH were co-injected with AAV1-
585 CMV-FLEX-SaCas9-U6-sgGrin1 to visualize GABA neurons and injection sites in the VTA.
586 Whole-cell recordings were performed on EGFP-positive GABA neurons with picrotoxin (100
587 µM) in the bath. NMDA components were measured as currents 20 ms after the peak at +40
588 mV, and AMPA components were measured as the peak at -70 mV. Previous literature
589 confirmed the absence of NMDA components without the obligatory GluN1 subunit[24,45,50].
590

C-Fos staining and immunohistochemistry

Drd1-Tomato mice were singly housed and habituated to handling and i.p. injections daily for seven days prior to the experiment. On the day of experiment, ketamine (30 mg/kg), cocaine (15 mg/kg) or saline (10 ml/kg) were injected i.p., mice were put back in their home cages and 90 min after the injections they were transcardially perfused under deep pentobarbital (150 mg/kg, i.p.) anesthesia. Brain sections were stained for c-Fos expression using standard immunohistochemistry. In brief, slices were incubated with primary antibody (1:5000, rabbit polyclonal anti-c-Fos, Synaptic Systems, 226 003) for 36 h at 4 °C and a secondary antibody (1:500, Alexa 488 goat anti-rabbit, Invitrogen, A1108) was used for visualization. Cell nuclei were stained with Hoechst (1:1000). Brain slices were imaged on a confocal microscope at 20x magnification and cells were counted manually by an experimenter blind to treatment.

Visualization of fiber location and protein expression

After fiber photometry experiments, mice were deeply anesthetized with pentobarbital (150 mg/kg, i.p.) and transcardially perfused with 4% paraformaldehyde. Fixed brains were cut in 50 µm thick slices and mounted on microscopy slides with mounting media containing DAPI. In some cases, to visualize of dLight expression or DA cells, we performed standard immunohistochemistry prior to slide mounting. In brief, slices were incubated with a primary antibody (1:500; for dLight: rabbit polyclonal anti-GFP, Invitrogen, A11122; for DA cells: mouse monoclonal anti-TH, Sigma, T2928) overnight at 4 °C and a secondary antibody (1:500, Alexa 488 goat anti-rabbit, Invitrogen, A1108 or Alexa 555 donkey anti-mouse, Invitrogen, A31570) was used for visualization. Cell nuclei in anti-GFP or anti-TH treated slices were stained with Hoechst (1:1000), instead of DAPI.

Statistics and reproducibility

Data were analyzed with Microsoft Excel 16.16.26 and GraphPad Prism 9. Sample size were estimated with G*power (HHU, Düsseldorf). Mice were randomly assigned to treatment conditions using an design of interleaved trials. Data were analyzed blind whenever possible. The experiments were replicated for at least two times and were successfully reproduced. Data were tested for normal distribution using the Shapiro-Wilk normality test. Normally distributed data sets were then tested with parametric comparisons, whereas non-parametric tests were chosen for non-normally distributed data sets. Post-hoc comparison was conducted if ANOVA yielded a significant main effect or interaction. Comparisons were two-tailed. Number of experimental replicates are noted in the figure legends. Details of statistical tests were shown in Supplementary Table 1.

Method References

49 Bariselli, S. *et al.* Role of VTA dopamine neurons and neuroligin 3 in sociability traits related to nonfamiliar conspecific interaction. *Nat Commun* **9**, 3173, doi:10.1038/s41467-018-05382-3 (2018).

50 Zweifel, L. S., Argilli, E., Bonci, A. & Palmiter, R. D. Role of NMDA receptors in dopamine neurons for plasticity and addictive behaviors. *Neuron* **59**, 486-496, doi:10.1016/j.neuron.2008.05.028 (2008).

51 Simmler, L. D. *et al.* Dual-action of ketamine confines addiction liability. Zenodo, https://doi.org/10.5281/zenodo.5772449 (2022).

Data availability

The datasets generated during and/or analyzed during the current study are available in the Zenodo repository, doi: 10.5281/zenodo.5772449[51].

Code availability

The Matlab code used for analyzing fiber photometry raw data is available in the Zenodo repository, doi: 10.5281/zenodo.5772449.

Funding and Disclosure

This study was supported by the Swiss National Science Foundation (L.D.S.; grant number PZ00P3_174178, C.L. 310030_189188) and the European Research Council (AdG F-Addict). The authors declare no competing interest.

Acknowledgements

The authors thank Jennifer Cand for laboratory assistance and Dr. Larry Zweifel from the University of Washington for providing the conditional NR1-KO and control viruses. We thank Alex Kwan, Camilla Bellone, and Manuel Mameli for their comments on an earlier version of the manuscript.

Author contributions

L.D.S. conceived experiments and performed patch recordings, fiber photometry, and behavioral experiments. Y.L. performed fiber photometry, patch recordings, and behavioral experiments. L.C.H. performed immunohistochemistry, fiber photometry, and behavioral experiments. A.H. performed mice surgeries and behavioral experiments. R.V.Z. performed fiber photometry experiments. L.D.S, Y.L., L.C.H., and R.V.Z. carried out analyses. C.L., L.D.S and Y.L. wrote the manuscript with the help of all authors. C.L. supervised the study.

Additional information

Extended Data information is available for this paper at Nature.

Correspondence and requests for materials should be addressed to C.L.

Reprints and permissions information is available at http://www.nature.com/ reprints.

Extended Data Fig. 1 | Lever presses and infusion intervals of self-administration. a, Lever presses on active and inactive lever during self-administration for each session. N (mice) = 8 (saline), 10 (ketamine), 8 (cocaine). **b,** Median inter-infusion interval per mouse in session 6 to estimate rate of infusion during non-contingent self-administration (**Fig. 3k**). N (mice) = 10 (ketamine), 7 (cocaine). Data are represented as mean ± SEM. *P < 0.05, **P < 0.01, ***P < 0.001.

Extended Data Fig. 2 | Dose-dependence of accumbal DA transients. a, Schematic of virus injection and fiber implantation targeting the medial shell of the nucleus accumbens. **b,** Mean dLight response to i.p. injections of different doses of ketamine. N = 5 mice. **c,** Area under the curve (AUC) from 0-10 min after i.p. injection of different doses of ketamine. N = 5 mice. Data are represented as mean ± SEM.

Extended Data Fig. 3 | Validation of NR1 ablation. a, Schematic of experimental details with virus injections and location of patch-clamp recordings. **b,** Representative traces of NMDA / AMPA recordings of NR1-KO (KO; sgGrin1) and control (CT; sgRosa26). Scale bar, 10 ms, 200 pA. **c,** NMDA / AMPA ratios (amplitudes measured for NMDA component 20 ms after the peak at +40 mV and AMPA component at -70 mV) of VTA GABA neurons from KO and CT mice. N (cells) = 6 (KO) and 6 (CT). Data are represented as mean ± SEM. *P < 0.05.

Extended Data Fig. 4 | Fentanyl and ketamine induced GABA inhibition and DA transients. a, c, e, Schematic of virus injection and fiber implantation. **b,** Mean Ca^{2+} signal of VTA GABA neurons from NR1-control (CT) and KO mice with i.p. injections of saline or fentanyl. N (mice) = 3 (CT) and 3 (KO). **d,** Average DA transients induced by ketamine (30 mg/kg) and fentanyl (0.3 mg/kg). N = 8 mice. **f,** Average DA transients induced by ketamine (30 mg/kg) and cocaine (15 mg/kg) in NR1-CT mice. N = 11 mice. **g,** Average DA transients induced by ketamine and cocaine in NR1-KO mice. N = 11 mice. Data are represented as mean ± SEM.

Extended Data Fig. 5 | In vitro NMDAR inhibition in acute brain slices of the NAc. a, Example traces of NMDAR EPSCs induced by electrical stimulation in the NAc, recorded in Mg^{2+}-free aCSF. Top: before bath-application of ketamine; bottom: with 50 µM ketamine. Stimulation artefact was removed. Scale bar is 50 ms, 50 pA. **b,** NMDAR EPSCs before and with ketamine. N = 5 cells. Data are presented as mean ± SEM. **P < 0.01.

Extended Data Fig. 6 | Compulsive ketamine self-administration and pain perception affected by ketamine infusions. a. Number of ketamine infusions in baseline and punishment sessions. N = 17 mice. **b.** Latency to hotplate before and after mocked saline and ketamine i.v. infusions (1 mg/kg/infusion, 30 infusions). N (mice) = 16 (saline) and 17 (ketamine). Data are presented as mean ± SEM. ***P < 0.001.

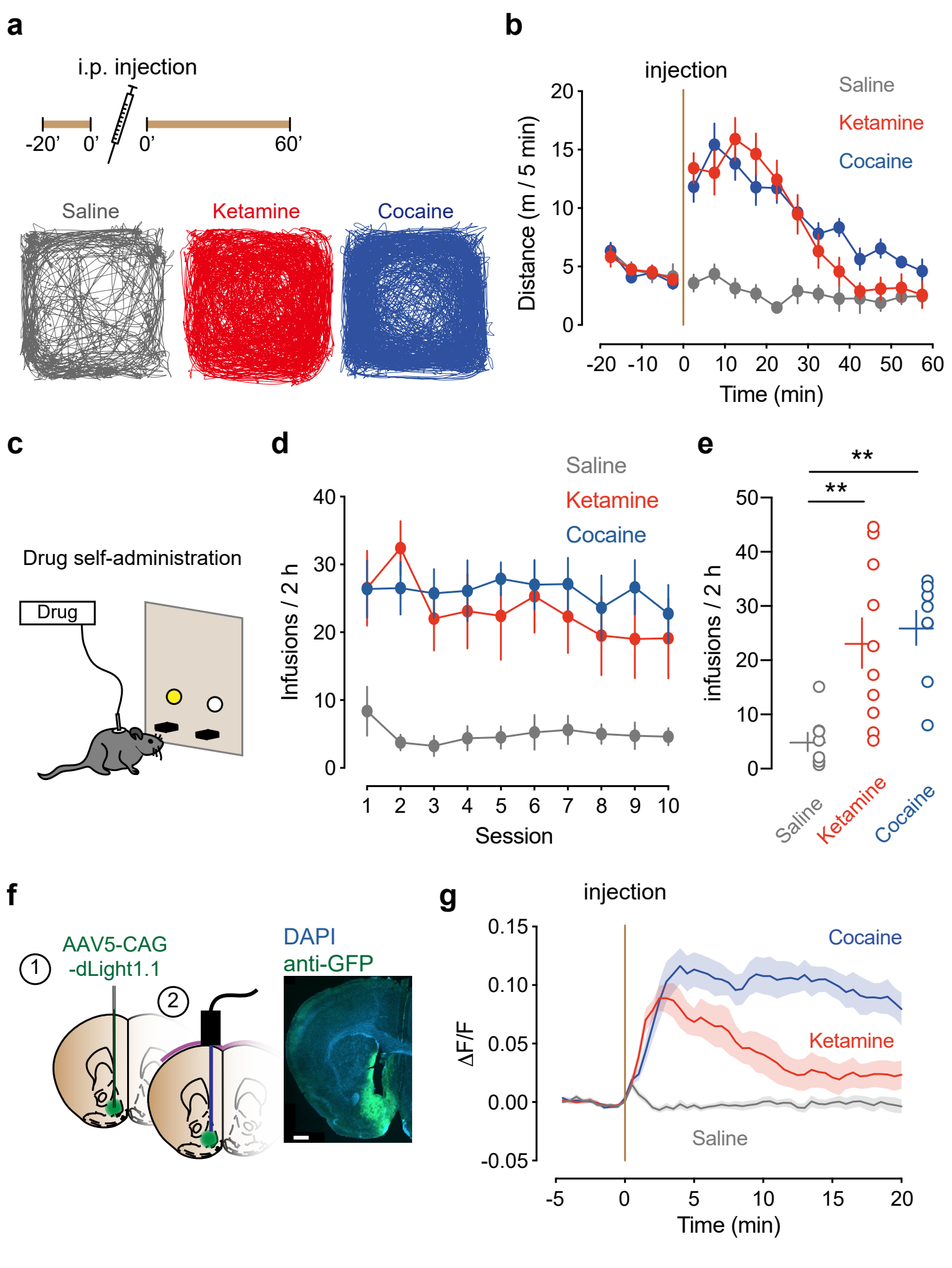
a
i.p. injection
-20'
0'
0'
60'
Saline
Ketamine
Cocaine
b
injection
Saline
Ketamine
Cocaine
Distance (m / 5 min)
Time (min)
c
Drug self-administration
Drug
d
Saline
Ketamine
Cocaine
Infusions / 2 h
Session
e
**
**
infusions / 2 h
Saline
Ketamine
Cocaine
f
AAV5-CAG
-dLight1.1
DAPI
anti-GFP
g
injection
Cocaine
Ketamine
Saline
ΔF/F
Time (min)

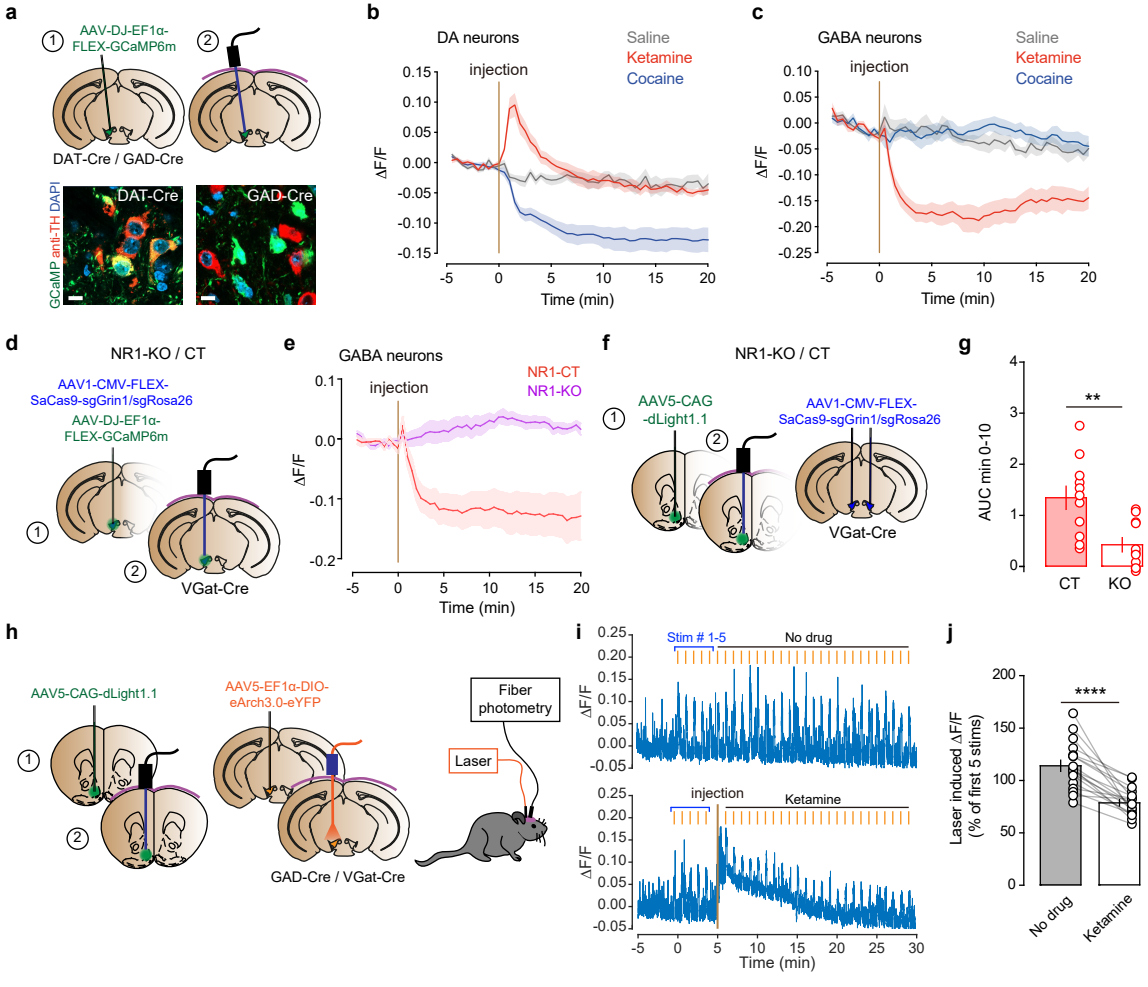
a
AAV-DJ-EF1α-
FLEX-GCaMP6m
DAT-Cre / GAD-Cre
DAT-Cre
GAD-Cre
GCaMP anti-TH DAPI
b
DA neurons
injection
Saline
Ketamine
Cocaine
ΔF/F
Time (min)
c
GABA neurons
injection
Saline
Ketamine
Cocaine
ΔF/F
Time (min)
d
NR1-KO / CT
AAV1-CMV-FLEX-
SaCas9-sgGrin1/sgRosa26
AAV-DJ-EF1α-
FLEX-GCaMP6m
VGat-Cre
e
GABA neurons
injection
NR1-CT
NR1-KO
ΔF/F
Time (min)
f
NR1-KO / CT
AAV5-CAG
-dLight1.1
AAV1-CMV-FLEX-
SaCas9-sgGrin1/sgRosa26
VGat-Cre
g
AUC min 0-10
**
CT
KO
h
AAV5-CAG-dLight1.1
AAV5-EF1α-DIO-
eArch3.0-eYFP
Fiber
photometry
Laser
GAD-Cre / VGat-Cre
i
Stim # 1-5
No drug
injection
Ketamine
ΔF/F
Time (min)
j
Laser induced ΔF/F
(% of first 5 stims)
****
No drug
Ketamine

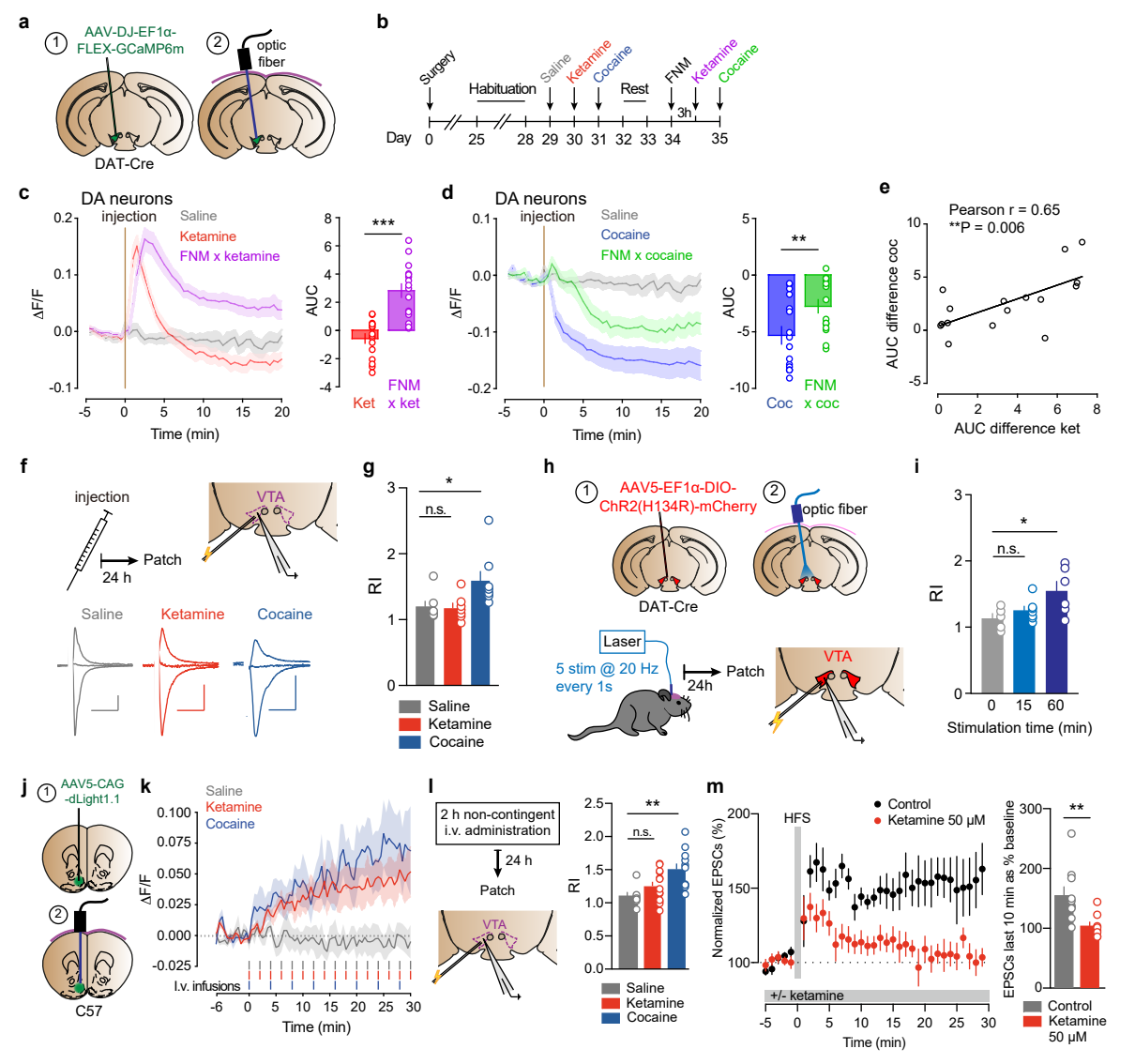
a
AAV-DJ-EF1α-FLEX-GCaMP6m
optic fiber
DAT-Cre
b
Surgery
Habituation
Saline
Ketamine
Cocaine
Rest
FNM
Ketamine
Cocaine
3h
Day 0 25 28 29 30 31 32 33 34 35
c
DA neurons
injection
Saline
Ketamine
FNM x ketamine
ΔF/F
Time (min)
AUC
***
Ket
FNM x ket
d
DA neurons
injection
Saline
Cocaine
FNM x cocaine
ΔF/F
Time (min)
AUC
**
Coc
FNM x coc
e
Pearson r = 0.65
**P = 0.006
AUC difference coc
AUC difference ket
f
injection
24 h
Patch
VTA
Saline
Ketamine
Cocaine
g
RI
*
n.s.
Saline
Ketamine
Cocaine
h
AAV5-EF1α-DIO-ChR2(H134R)-mCherry
optic fiber
DAT-Cre
Laser
5 stim @ 20 Hz every 1s
24h
Patch
VTA
i
RI
*
n.s.
Stimulation time (min)
j
AAV5-CAG -dLight1.1
C57
k
Saline
Ketamine
Cocaine
ΔF/F
I.v. infusions
Time (min)
l
2 h non-contingent i.v. administration
24 h
Patch
VTA
RI
**
n.s.
Saline
Ketamine
Cocaine
m
HFS
Control
Ketamine 50 μM
Normalized EPSCs (%)
+/- ketamine
Time (min)
EPSCs last 10 min as % baseline
**
Control
Ketamine 50 μM

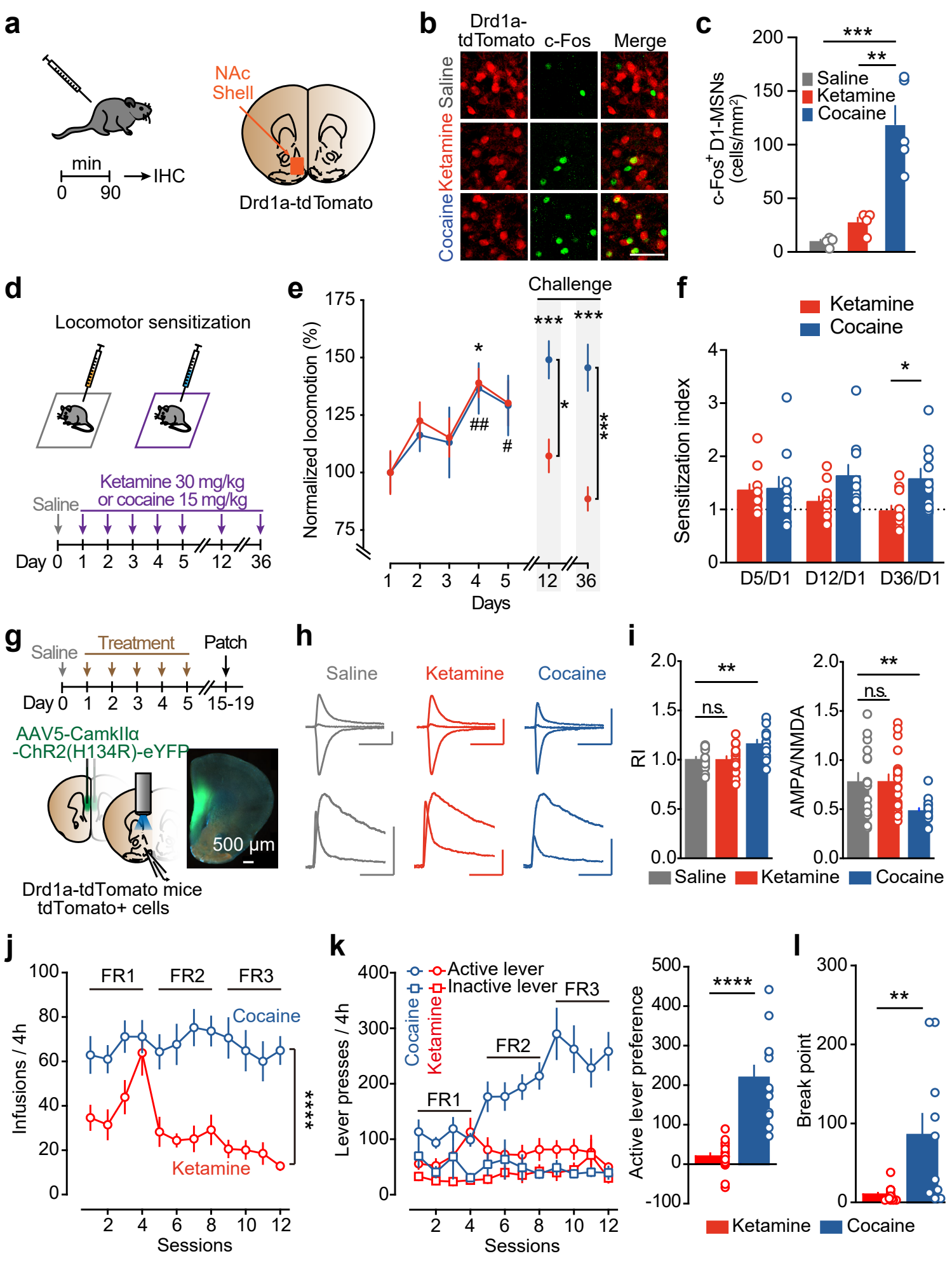
a
min
0
90
IHC
NAc
Shell
Drd1a-tdTomato
b
Drd1a-
tdTomato
c-Fos
Merge
Saline
Ketamine
Cocaine
c
c-Fos+ D1-MSNs
(cells/mm2)
Saline
Ketamine
Cocaine
***
**
d
Locomotor sensitization
Ketamine 30 mg/kg
or cocaine 15 mg/kg
Saline
Day 0 1 2 3 4 5 12 36
e
Challenge
Normalized locomotion (%)
Days
*
##
#
***
f
Ketamine
Cocaine
Sensitization index
D5/D1
D12/D1
D36/D1
g
Saline
Treatment
Patch
Day 0 1 2 3 4 5 15-19
AAV5-CamkIIα
-ChR2(H134R)-eYFP
500 μm
Drd1a-tdTomato mice
tdTomato+ cells
h
Saline
Ketamine
Cocaine
i
RI
AMPA/NMDA
n.s.
Saline
Ketamine
Cocaine
j
FR1
FR2
FR3
Cocaine
Ketamine
Infusions / 4h
Sessions
****
k
Active lever
Inactive lever
Cocaine
Ketamine
Lever presses / 4h
Active lever preference
Sessions
l
Break point
Ketamine
Cocaine